

Sturmian theory of three-body recombination

Robert C. Forrey

Department of Physics, Penn State University, Berks Campus, Reading, PA 19610-6009

(June 6, 2019)

Abstract

A Sturmian theory of three-body recombination is presented which provides a unified treatment of bound states, quasi-bound states, and continuum states. The Sturmian representation provides a numerical quadrature of the two-body continuum which may be used to generate a complete set of states within any desired three-body recombination pathway. Consequently, the dynamical calculation may be conveniently formulated using the simplest energy transfer mechanism, even for reactive systems which allow substantial rearrangement. For a three atom system which is not in thermal equilibrium, the steady-state recombination rate constants are shown to be weakly dependent on tunneling widths and pressure. Numerical results are presented for H_2 recombination due to collisions with H and He using quantum mechanical coupled states and infinite order sudden approximations. These results may be used to remove some of the uncertainties that are currently limiting astrophysical simulations of primordial star formation.

I. INTRODUCTION

Three-body recombination (TBR) is one of the most fundamental types of chemical reaction and has a long history of study (see [1] and references therein). Probably, the most widely used approach to computing TBR rates is the orbiting resonance theory (ORT) developed by Roberts, Bernstein, and Curtiss (RBC) [2]. In this theory, recombination occurs through a sequential two-step process where the first step consists of the formation of a quasibound (QB) orbiting resonance state of a two-body subsystem. The second step transfers the QB state to a bound state through either an energy transfer (ET) process or an exchange (Ex) process. For both two-step mechanisms, the QB states are assumed to have sufficiently short lifetimes that they maintain equilibrium with the free atomic states.

A quantum kinetic theory of chemical recombination was later developed by Snider and Lowry [3] which removed the *assumption* of equilibrium between the monomers and dimers. The result appeared to be the same as that of ORT with the exception that the sum over intermediate QB states in the ORT formulation be replaced by a complete set of intermediate states. Because the intermediate states are not considered to be independent molecular species, there is some flexibility in the choice of pathway for the TBR process. This flexibility was emphasized by Wei, Alavi, and Snider [4] who formally proved that all pathways (including direct 3-body collisions) must yield the same rate constant when the sum over two-body states is complete, and cautioned that adding partial results from different pathways could lead to double counting of some of the transition probability.

In practice, however, the pathway independence has not proven to be of great utility. Classical dynamical calculations, which are included in the bulk of TBR studies, generally do not distinguish between free particle states and the interacting continuum. Quantum calculations which do make this distinction have found it difficult to include broad above barrier (BAB) resonances and the non-resonant continuum within the ET mechanism due to the dynamical requirement that the states be square integrable. An attempt in this direction was made by Pack, Walker, and Kendrick [1] who tried to use an L^2 representation of the BAB resonances. They found unsatisfactory results because the wave functions for these

resonances are less localized, and their results depended on the number of nodes that were included in the representation. It was concluded that the BAB resonances and non-resonant continuum could not in practice be included in any accurate quantum calculations of the ET mechanism, and therefore, the contributions from these states to TBR were treated and included separately [1].

This conclusion was premature, however, as it was based on fitting, truncating, and normalizing L^2 functions to numerical wave functions obtained from scattering calculations. If instead the L^2 functions were computed as positive energy eigenfunctions of a Sturmian representation of the two-body Hamiltonian, then the apparent arbitrariness in truncating the L^2 functions found in [1] might be removed. The positive energy eigenfunctions would provide a quadrature of the continuum which would give a unified treatment of all QB, BAB, and non-resonant continuum states and allow convergence tests to be performed. This approach was used by Paolini, Ohlinger, and Forrey [5] to compute TBR rates for H_2 due to collisions with He and Ar. The results appeared promising and confirmed the importance of non-resonant contributions to recombination observed in earlier works [6,7]. However, discrepancies remained when the theoretical results were compared to existing experimental data. In an effort to resolve these discrepancies, it was shown [5] that a model steady-state approximation at high pressure could be used to adjust the theoretical results and bring them into agreement with the experiment.

In general, a steady-state approximation should be more accurate than an equilibrium approximation. However, the steady-state approximation that is conventionally used and which was used in [5] neglects the repopulation of intermediate molecules by three-body collisions. In this approximation, the ORT contribution to recombination rapidly decreases at high pressure due to a depleted concentration of metastable QB states. A master equation analysis performed by Pack, Walker, and Kendrick [6] showed that three-body collisions can effectively keep the metastable QB states from being depleted at high pressure. In their study of Ne_2 recombination due to collision with H, they found only a small change ($\sim 7\%$) in the recombination rate over a large range of pressure. In the Sturmian theory presented here,

we show that the pressure dependence completely vanishes for three-body systems whose internal states are in thermal equilibrium, and confirm the weak dependence on tunneling widths and pressure that is found [6–8] in the more general case. The QB contributions to the TBR rate do not vanish for large lifetimes as is generally assumed in the RBC procedure of discarding long-lived QB states [2], and the weak dependence on tunneling widths and pressure shows that the conventional steady-state approximation used in [5] to adjust the theory to the experimental data is not justified.

A practical benefit of the Sturmian theory is the ability to take advantage of the pathway invariance of the TBR rate. This allows the dynamical calculation to be formulated in terms of the simplest process, which is usually the ET mechanism. Unlike many calculations in the literature which add the QB contributions of the ET and Ex mechanisms together with the direct 3-body contributions, the ET mechanism is all that is required in the Sturmian theory at equilibrium. The Sturmian representation of the intermediate states provides a numerical implementation of the quantum kinetic theory of Snider and Lowry [3] which ensures that there are no problems associated with double counting of the kind described by Wei, Alavi, and Snider [4].

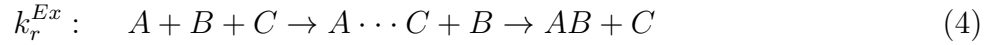
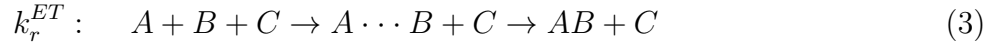
The theory is applied to the calculation of TBR rates for $\text{He}+\text{H}+\text{H}$ and $\text{H}+\text{H}+\text{H}$, two systems which have been well-studied in the past [2,9–14] but which still have significant uncertainties that limit the reliability of current astrophysical simulations of primordial star formation [15]. In order to make use of the Sturmian representation, we also use a quantum mechanical formulation of the three-body dynamics. At the relatively high temperatures required by the astrophysical simulations, the quantum mechanical formulation is mainly needed for identification of the collision complex and for ensuring that there is no double counting. The dimensionality of the quantum mechanical set of coupled equations may be reduced through angular momentum decoupling approximations. A comparison of results obtained using the coupled states (CS) and infinite order sudden (IOS) approximations is made, and the reliability of each result is discussed. The results may be used to remove some of the uncertainty in the TBR rates that have been used in the astrophysical models.

II. THEORY

We begin by considering a system of three atoms A, B, and C whose internal atomic and molecular states are in thermal equilibrium. We wish to calculate the rate constants in the effective rate equation

$$[C]^{-1} \frac{d}{dt} [AB] = k_r [A][B] - k_d [AB] \quad (1)$$

where the square brackets denote number density of the enclosed species, and k_r and k_d are the respective rate constants for TBR and collision induced dissociation (CID). If the internal states are not in equilibrium, then the rate constants will not actually be constant in time, but may be defined as the coefficients of a steady-state solution to equation (1). Recombination of two atoms A and B to form molecule AB may occur through a direct pathway with rate k_r^0 or through an indirect pathway with rate k_r^{ET} or k_r^{Ex} as shown



with the corresponding transition operators [4]

$$T_0 = (V - v_{AB})(1 + G_E^+ V) \quad (5)$$

$$T_{ET} = (V - v_{AB}) \left[1 + G_E^+ (V - v_{AB}) \right] \Omega_{AB} \quad (6)$$

$$T_{Ex} = (V - v_{AB}) \left[1 + G_E^+ (V - v_{AC}) \right] \Omega_{AC} \quad (7)$$

where G_E^+ is the outgoing wave Green's function for the full Hamiltonian consisting of the three-body potential V and the total kinetic energy operator KE . The potentials v_{AB} and v_{AC} refer to two-body interactions, and

$$\Omega_{AB} = 1 + (E^+ - KE - v_{AB})^{-1} v_{AB} \quad (8)$$

is the Moller operator which connects the free continuum with the interacting continuum. In the ORT formulation, the (\cdots) notation refers to metastable QB orbiting resonance states,

and the recombination rate constant is commonly assumed to be $k_r = k_r^0 + k_r^{ET} + k_r^{Ex}$. An additional exchange mechanism may be included for intermediate $B \cdots C$ states if desired. Wei, Alavi, and Snider have shown [4] that when the (\cdots) notation instead refers to a complete set of interacting two-body states, the recombination rate constant is $k_r = k_r^0 = k_r^{ET} = k_r^{Ex}$. The Sturmian theory provides such a complete set and allows the dynamical calculation to be formulated entirely in terms of any one of the above mechanisms.

The TBR and CID rate constants may be defined so that the quantum kinetic theory of Snider and Lowry [3] is recovered for a system in local thermodynamic equilibrium (LTE)

$$k_r \equiv \sum_{b,u} k_{u \rightarrow b} \frac{[AB(u)]}{[A][B]} \Rightarrow \sum_{b,u} k_{u \rightarrow b} \frac{g_u \exp(-E_u/k_B T)}{Q_A Q_B Q_T} \text{ at LTE} \quad (9)$$

$$k_d \equiv \sum_{b,u} k_{b \rightarrow u} \frac{[AB(b)]}{[AB]} \Rightarrow \sum_{b,u} k_{b \rightarrow u} \frac{g_b \exp(-E_b/k_B T)}{Q_{AB}} \text{ at LTE} \quad (10)$$

where b designates a bound state with energy E_b and u designates an unbound state with energy E_u . If the direct mechanism (2) is used to formulate the dynamics, then u must be a free continuum state, whereas the indirect mechanisms (3) and (4) would require that u correspond to an interacting continuum state. In order to avoid confusion, we will use f to designate a free continuum state and u to designate an interacting continuum state. The atomic and molecular partition functions are Q_A , Q_B , and Q_{AB} , respectively. The translational partition function Q_T is defined by

$$Q_T = \frac{1}{h^3} \int_0^\infty \exp\left(-\frac{p^2}{2mk_B T}\right) 4\pi p^2 dp = \frac{(2\pi m k_B T)^{3/2}}{h^3} \quad (11)$$

where m is the reduced mass of AB , h is Planck's constant, k_B is Boltzman's constant, and T is the temperature. The discrete sum over unbound states in equations (9) and (10) is a mathematically rigorous approximation for a Sturmian basis set whose eigenstates represent quadrature points of the continuum. This may be verified numerically by using the free energy eigenvalues to compute the integral in equation (11)

$$Q_T = \frac{4\pi m}{h^3} \sum_f w_f \sqrt{2mE_f} \exp(-E_f/k_B T) \quad (12)$$

where w_f are the equivalent quadrature weights [16] of the chosen Sturmiian representation.

The rate coefficients are defined in the usual way as

$$k_{i \rightarrow j} = \left(\frac{8k_B T}{\pi \mu} \right)^{1/2} (k_B T)^{-2} \int_0^\infty \sigma_{i \rightarrow j}(E_T) \exp(-E_T/k_B T) E_T dE_T \quad (13)$$

where μ is the reduced mass of an atom with respect to a diatom, and $E_T = E - E_i$ is the translational energy in the i th channel, which may be taken to be bound or unbound. For the indirect mechanisms (3) and (4), the collision cross section $\sigma_{i \rightarrow j}$ refers to non-reactive and reactive atom-diatom scattering, respectively. Applying the principle of detailed balance

$$k_{j \rightarrow i} = \frac{g_i}{g_j} \exp\left(\frac{E_j - E_i}{k_B T}\right) k_{i \rightarrow j} \quad (14)$$

to the LTE limit of equations (9) and (10) yields the statistical Saha equation

$$\frac{k_r}{k_d} = \frac{[AB]}{[A][B]} = \frac{Q_{AB}}{Q_A Q_B Q_T} = (Q_A Q_B Q_T)^{-1} \sum_b g_b \exp(-E_b/k_B T) \quad (15)$$

for the thermalization of the continuum.

For a system which is not in thermal equilibrium, a more detailed rate analysis is required.

The effective rate equation (1) may be replaced by a set of state-specific rate equations

$$\begin{aligned} \frac{d}{dt}[AB(b)] &= [C] \sum_u (k_{u \rightarrow b}[AB(u)] - k_{b \rightarrow u}[AB(b)]) \\ &\quad + [C] \sum_{b'} (k_{b' \rightarrow b}[AB(b')] - k_{b \rightarrow b'}[AB(b)]) \end{aligned} \quad (16)$$

$$\begin{aligned} \frac{d}{dt}[AB(u)] &= [C] \sum_b (k_{b \rightarrow u}[AB(b)] - k_{u \rightarrow b}[AB(u)]) + k_{f \rightarrow u}^{elastic}[A][B] \\ &\quad + [C] \sum_{u'} (k_{u' \rightarrow u}[AB(u')] - k_{u \rightarrow u'}[AB(u)]) - \tau_u^{-1}[AB(u)] \end{aligned} \quad (17)$$

where τ_u is the lifetime of the unbound state u , and $k_{f \rightarrow u}^{elastic}$ is the two-body elastic scattering rate constant for the reverse process which may be computed from τ_u^{-1} using the equilibrium constant K_u^{eq} . The steady-state solution to equation (17) is given by

$$\frac{[AB(u)]}{[A][B]} = \frac{K_u^{eq} + \tau_u [C] [A]^{-1} [B]^{-1} \left(\sum_b k_{b \rightarrow u}[AB(b)] + \sum_{u' \neq u} k_{u' \rightarrow u}[AB(u')] \right)}{1 + \tau_u [C] \left(\sum_b k_{u \rightarrow b} + \sum_{u' \neq u} k_{u \rightarrow u'} \right)} \quad (18)$$

In the conventional steady-state approximation, the CID contribution $k_{b \rightarrow u}$ is assumed to be small due to the excitation threshold, and the $k_{u' \rightarrow u}$ contribution in the numerator of

equation (18) is neglected for no particularly good reason. It is precisely this term that Pack, Walker, and Kendrick [6] discovered in their master equation analysis which keeps the QB states from being depleted at high pressures. When it is neglected, the numerator of equation (18) would approximately equal K_u^{eq} and $[AB(u)]$ would appear to be very small for long-lived QB states and high concentrations $[C]$. When this steady-state result is used to obtain the ORT recombination rate, there would be a substantial falloff at high pressures. As noted in [6], such strong ORT “falloff” is not generally observed in experiments.

A better approach is to solve the full set of master equations (16) and (17) to obtain steady-state concentrations. It is convenient to write equations (9) and (10) as

$$k_r \equiv \sum_{b,u} (1 + \delta_u) k_{u \rightarrow b} \frac{g_u \exp(-E_u/k_B T)}{Q_A Q_B Q_T} \quad (19)$$

$$k_d \equiv \sum_{b,u} (1 + \delta_b) k_{b \rightarrow u} \frac{g_b \exp(-E_b/k_B T)}{Q_{AB}} \quad (20)$$

and express the solution of the master equations in terms of the pathway-independent LTE part plus a term containing the non-LTE concentration defects

$$\delta_u = \frac{\tau_u [C] \left(\sum_b \delta_b k_{u \rightarrow b} + \sum_{u' \neq u} \delta_{u'} k_{u \rightarrow u'} \right)}{1 + \tau_u [C] \left(\sum_b k_{u \rightarrow b} + \sum_{u' \neq u} k_{u \rightarrow u'} \right)} \quad (21)$$

$$\delta_b = \frac{\sum_{b'} \delta_{b'} \Gamma_{b \rightarrow b'} + [C] \left(\sum_u \delta_u k_{b \rightarrow u} + \sum_{b' \neq b} \delta_{b'} k_{b \rightarrow b'} \right)}{\sum_{b'} \Gamma_{b \rightarrow b'} + [C] \left(\sum_u k_{b \rightarrow u} + \sum_{b' \neq b} k_{b \rightarrow b'} \right)} \quad (22)$$

where $\Gamma_{b \rightarrow b'}$ has been added to allow for radiative transitions. Note that the LTE part of the rate constants (19) and (20) does not depend on pressure. The non-LTE concentration defects allow for QB states that have lifetimes that are long enough to survive a three-body collision or are formed through an independent process. These defects are typically small and negative. Equations (21) and (22) refer to the ET mechanism, but it is here that any important exchange mechanisms may also be included in the kinetics (see below).

Equation (19) has much in common with the kinetic model proposed in [6]. At low pressures and short lifetimes, the δ_u makes a negligible contribution and the recombination rate is simply equal to the pathway-independent LTE result. Note that in this limit, the QB

states still contribute when an indirect mechanism is used to compute the rate constant. At high pressure, the δ_u becomes important for QB states with large lifetimes. Equation (21) shows that when the defects δ_b and $\delta_{u'}$ are negative, the pressure-dependent QB contribution gets subtracted from the pathway independent part. This provides a small “falloff” to the recombination rate of the kind observed in [6] where the low and high pressure limits differed by only $\sim 7\%$. This small falloff compared to ORT is due to a combination of the inclusion of short-lived u -states and the incomplete removal of long-lived u -states in equation (19).

A similar result is obtained when the system allows a QB state of the $A \cdots C$ complex. In this case, the δ_u in equations (19) and (21) are simply replaced by

$$\delta_u^{AB} = \frac{\tau_u^{AB}[C] \left\{ \sum_b (\delta_b^{AB} k_{u \rightarrow b}^{ET} + \delta_b^{AC} k_{u \rightarrow b}^{Ex}) + \sum_{u' \neq u} (\delta_{u'}^{AB} k_{u \rightarrow u'}^{ET} + \delta_{u'}^{AC} k_{u \rightarrow u'}^{Ex}) \right\}}{1 + \tau_u^{AB}[C] \left\{ \sum_b (k_{u \rightarrow b}^{ET} + k_{u \rightarrow b}^{Ex}) + \sum_{u' \neq u} (k_{u \rightarrow u'}^{ET} + k_{u \rightarrow u'}^{Ex}) \right\}} \quad (23)$$

with the superscripts AB and AC used to clarify the lifetime and concentration defects, and the superscripts ET and Ex used to denote a direct or exchange collision. This expression is easily generalized for systems which also allow a QB state of the $B \cdots C$ complex. The key point is that the pathway-independent LTE rate coefficient does not depend on pressure and provides the largest contribution to the full pressure-dependent rate k_r . Any pressure dependence which might arise from long-lived QB states should not be simply added to a direct pathway rate as is commonly done in the literature. Instead, such contributions should be subtracted from the pathway-independent part with weights obtained via solution of the master equations. Typically, the non-LTE defects are small, so if a master equation analysis is not performed, it is usually best to set the defects to zero and use only the pathway-independent part.

Perhaps the most significant advantage in using the Sturmian theory to compute TBR rates is that it allows the pathway-independent part of the rate coefficients (19) and (20) to be calculated entirely in terms of the ET mechanism. The dynamics for these rate coefficients then reduces to non-reactive scattering calculations which are generally easier to deal with than the reactive scattering calculations that would be needed to formulate the theory in terms of the Ex mechanism. In cases where there is strong interference between reactive and non-reactive channels, this may not amount to much of an advantage as any quantum

dynamical calculation would require a full account of all arrangement channels. This would likely be the case for attractive systems at low temperatures. However, for temperatures that are high enough that classical trajectories would permit a good approximation to the dynamics, any quantum interference between the reactive and non-reactive channels would be unimportant, and the non-reactive channels could be separated out. In this case, it is still desirable to perform quantum dynamical calculations in order to utilize the Sturmian basis set and avoid the double counting problems discussed by Wei, Alavi, and Snider [4].

A quantum mechanical calculation of the collision cross section needed in equation (13) may be obtained by considering the atom-diatom Hamiltonian in the center of mass frame

$$H = -\frac{1}{2m} \nabla_r^2 - \frac{1}{2\mu} \nabla_R^2 + v(r) + V_I(r, R, \theta) \quad (24)$$

where r is the distance between atoms A and B , R is the distance between atom C and the center of mass of $A \cdots B$, θ is the angle between r and R , m and μ are defined as above, and the three dimensional potential energy surface is separated into a diatomic potential $v(r)$ and an interaction potential $V_I(r, R, \theta)$. The first step of the ET mechanism requires solution of the diatomic Schrödinger equation

$$\left[\frac{1}{2m} \frac{d^2}{dr^2} - \frac{j(j+1)}{2m r^2} - v(r) + E_{vj} \right] \chi_{vj}(r) = 0, \quad (25)$$

where v and j are the vibrational and rotational quantum numbers for the eigenstate χ_{vj} . The bound ro-vibrational wave functions and discretized positive energy states are obtained by diagonalization of the diatomic Hamiltonian in an orthonormal L^2 Sturmian basis set. In the coupled channel (CC) method, the full wave function is expanded in terms of channel functions $n \equiv \{v, j, l\}$ which leads to a set of equations

$$\left[\frac{d^2}{dR^2} - \frac{l_m(l_m+1)}{R^2} + k_m^2 \right] C_m(R) = 2\mu \sum_n C_n(R) \langle \phi_m | V_I | \phi_n \rangle \quad (26)$$

where l_m is the orbital angular momentum in the m -th channel and $k_m^2 = 2\mu(E - E_m)$ is the square of the translational wave number. Because the positive energy eigenstates in the Sturmian representation correspond to quadrature points of the two-body continuum [16], the uncountably infinite set of continuum states is coupled together in an approximation

scheme which mirrors what is usually done for calculating transitions between bound states. Therefore, it should be possible to compute TBR rate coefficients using the numerically exact CC method for systems which do not require coupling to states with large values of j . The dimensionality of the set of coupled equations grows rapidly with increasing j due to the exact treatment of the angular momentum coupling, so it is also desirable to consider various decoupling approximations. One of the most reliable decoupling approximations is the coupled states or centrifugal sudden (CS) approximation [17–19] which replaces the m -th channel orbital angular momentum l_m with an average value \bar{l} and reduces the channel index to include only the state quantum numbers v and j . The infinite-order-sudden (IOS) approximation [20] makes the additional approximation that the internal rotational energy is averaged over so that the orientation angle θ is treated as a parameter. A more severe IOS approximation [21] averages over both the internal rotational and vibrational energy so that the set of coupled equations (26) reduces to a set of uncoupled one-dimensional equations. This version was used by Pack et al. [1] to study TBR of Ne_2 due to collisions with H, and it was estimated to be accurate to within about 20% at low temperatures (~ 30 K) due to the closely spaced energies. The internal energies for H_2 are not as closely spaced, however, the spacing decreases with excitation, and for the most important transitions to highly excited states, the approximation is expected to give semiquantitative accuracy [22] which improves as the translational temperature increases. Therefore, the IOS results reported in this work correspond to this most simplified version of the approximation.

Various reactive IOS approximations have also been developed [23] and applied to $\text{H}+\text{H}_2$ collisions [24–27]. In the reactive IOS with optical potential [28], the problem reduces to a non-reactive formulation for a single arrangement. Similarly, an L^2 Sturmian representation of the ET mechanism is able to convert a multi-arrangement system into an inelastic single arrangement system. However, negative imaginary potentials cannot be used to absorb large- r flux due to the free three-body boundary condition. Instead, the convergence of the Sturmian method relies on the square integrability of the basis set. For reactive systems, the CC and CS formulations typically require that all basis functions used to represent

the free and interacting continuum be coupled together in the dynamics. This will almost always present an insurmountable practical limitation. The IOS approximation, however, decouples the internal coordinates and allows a practical solution. Furthermore, when the Sturmian basis set is used within the IOS approximation, the energy thresholds for the unbound states are exactly handled and the cross sections exactly satisfy the principle of microscopic reversibility. Therefore, the rate coefficients exactly satisfy detailed balance, which is essential to the kinetic analysis given above.

III. RESULTS

The pathway-independent part of the TBR rate constant (19) is calculated for He+H+H and H+H+H using the ET mechanism. In both cases, the H₂ potential is obtained using a fit [29] to the Ad potential of Schwenke [30]. The MR PES [31] and also an additive pair potential PES were separately used for the HeH₂ system. The BKMP2 PES [32] was used for the H₃ system. For light atomic systems, such as the hydrogen pairs considered here, it is convenient to use a Sturmian representation consisting of Laguerre polynomial $L_n^{(2j+2)}$ basis functions

$$\phi_{j,n}(r) = \sqrt{\frac{an!}{(n+2j+2)!}} (ar)^{j+1} \exp(-ar/2) L_n^{(2j+2)}(ar) . \quad (27)$$

In this work, we included $n = \{0, \dots, 100\}$ for each value of $j \leq 35$. The diatomic Schrödinger equation (25) was solved numerically using this basis set for both the free particle interaction $v = 0$ and the full two-body interaction for H₂. The accuracy of the Sturmian representation may be assessed by its ability to reproduce the translational partition function Q_T using the free particle energy eigenvalues as given by equation (12). The equivalent quadrature weights w_f were computed as numerical derivatives of the discrete energy eigenvalues with respect to index number [16] using a spline fit. Figure 1a shows the percent error between equations (11) and (12) for different values of scale parameter a . The Sturmian eigenvalues in this plot are associated with $j = 4$, however, the pattern is similar for all j . For the 101 basis functions used here, the accuracy of the Sturmian representation of Q_T is seen to be

best for the smallest scale factor shown. The accuracy of the interacting eigenvalues, whose bound and QB states are governed by a variational principle, is also affected by the choice of scale parameter, so an appropriate balance between the two is desirable and deserving of further study. Figure 1b shows the percent error using equation (12) with the positive energy eigenvalues of the interacting continuum. The calculations were performed both with and without the long-lived $j = 4$ QB state ($\tau \sim 6 \times 10^{-7}$ sec) included in the summation. At high temperatures, the interacting continuum which includes the QB state in the summation gives a better approximation to the translational partition function.

Figure 2 shows the 14th vibrational eigenstate for a $j = 4$ Sturmian representation of the free and interacting continuum of $\text{H} \cdots \text{H}$ using a scale parameter $a = 20$. Note that the vibrational quantum number for a positive energy eigenstate corresponds to the quadrature index and only has meaning with respect to the scale parameter. In both cases, the eigenstate is plotted versus interatomic distance using the normalization

$$\psi = \frac{\chi_{vj}(r)}{\sqrt{w_{vj}}} \Rightarrow \sqrt{\frac{2m}{\pi k_{vj}}} k_{vj} r j_l(k_{vj} r) \quad \text{for free continuum} \quad (28)$$

where $k_{vj} = \sqrt{2mE_{vj}}$ and j_l is a spherical Bessel function. As may be seen in Figure 2a, the Sturmian representation shows excellent agreement with the exact free continuum state for $r \leq 20$ a.u. before going quickly to zero as required by the exponential term in the basis functions. All of the free and interacting continuum states are cut off at the same distance. This cut-off distance is not an arbitrary choice, but is instead controlled by the choice of scale parameter. The interacting eigenstate shown in Figure 2b corresponds to a long-lived QB state with tunneling width $\Gamma \sim 8 \times 10^{-6} \text{ cm}^{-1}$ and resonant energy $E_r \sim 0.9 \text{ cm}^{-1}$.

Another long-lived QB state is shown in Figure 3 for $j = 15$ and $v = 13$. Also shown in the figure are wavefunctions for the non-resonant $v = 12$ and $v = 14$ states. The QB state ($\Gamma \sim 3 \times 10^{-6} \text{ cm}^{-1}$ and $E_r \sim 190 \text{ cm}^{-1}$) is localized below 10 a.u. which produces a strong contribution to the TBR rate. Clearly, there is negligible overlap between the QB state and the neighboring continuum. Higher vibrational levels do show more significant overlap and can help keep the QB concentration from being depleted at high pressures. The pressure dependence of this resonant contribution to the TBR rate is examined below.

Figure 4 shows the cumulative bound-free transition probability as a function of the positive energy Sturmian eigenvalues. The calculations are for $\text{He}+\text{H}\cdots\text{H}(j=4)$ computed in the IOS approximation using the MR PES [31]. The curves shown in the figure include a summation of the state-to-state probabilities over all bound states, and each point was computed with $E_T^{(u)} = 100 \text{ cm}^{-1}$ and $J_{max} = 30$. The state-to-state probabilities, which are defined as

$$P_{b\leftrightarrow u}(E) = \left(\frac{2\mu E_T^{(b)}}{\pi} \right) g_b \sigma_{b\rightarrow u}(E_T^{(b)}) = \left(\frac{2\mu E_T^{(u)}}{\pi} \right) g_u \sigma_{u\rightarrow b}(E_T^{(u)}) \quad (29)$$

have a scale dependence when computed using the Sturmian eigenstates. This is due to the unit normalization of the L^2 basis functions. We could easily energy-normalize the Sturmian eigenstates as was done in equation (28). However, we are only interested in the sum of the probabilities over u -states, so it is not necessary to energy-normalize these states. The weights w_f needed for a quadrature of the free continuum cancel with the weights in equation (28). The Moller operator converts the sum over f -states to a sum over u -states, so we can simply add together the values at the energy eigenvalues shown in the figure. When this is done for $E_u < 37,500 \text{ cm}^{-1}$, the results for the four different scale parameters give excellent agreement, particularly for $a = 10 - 30$. In the figure, all four curves clearly show the resonant contribution as the lowest energy quadrature point. The resolution of this resonant contribution is best for the small scale parameters due to their closer spacing of energy eigenvalues. The larger scale parameters provide larger spacing which enables the quadrature to include higher energies. In the present work, we found it convenient to use $a = 20$ for all IOS calculations.

Figure 5 shows partial TBR rate constants for $\text{He}+\text{H}\cdots\text{H}(j=15)$ computed using the IOS approximation with the MR PES [31]. Each curve includes a sum over all bound levels. The BAB resonance gives a contribution which is comparable to the discretized states of the non-resonant continuum. The low energy non-resonant states corresponding to $v = 14 - 20$ give contributions which range over several orders of magnitude, whereas the higher energy $v = 22 - 25$ states give contributions with less variation but with a gradual shift in threshold energy. The sharp QB resonance gives more than an order of magnitude larger contribution

than any of the other $j = 15$ states. This is due to the strong localization of the QB state at short distances and the negligible overlap with neighboring continuum states (see Figure 3). In order to study the effect of pressure on this QB contribution to the TBR rate constant, we estimated the non-LTE concentration defect δ_u given in equation (21) using the IOS rate coefficients $k_{u \rightarrow b}$ and $k_{u \rightarrow u'}$. The maximum possible pressure-dependence would occur when $\delta_b = -1$ which corresponds to zero concentration of bound level b . We assume $\delta_{u'} = 0$ which should be a good approximation for BAB resonances and the non-resonant background [6]. For QB states where $\delta_{u'} \neq 0$, the rate coefficient connecting u' with u is typically small enough that the $\delta_{u'} = 0$ assumption would not substantially effect our estimate. The result is $\delta_u = -0.44$ in the $[\text{He}] \rightarrow \infty$ limit. This defect provides the maximum amount of falloff with pressure that can occur for this QB state. Tables I and II show the maximum defects δ_u^{max} for all QB states with tunneling widths less than 0.01 cm^{-1} . Also given in the tables is the critical density of He atom colliders, defined by

$$[\text{He}]_{cr} = \frac{1}{\tau_u \left(\sum_b k_{u \rightarrow b} + \sum_{u' \neq u} k_{u \rightarrow u'} \right)} \quad (30)$$

which gives an estimate of where the falloff would be expected to occur. Not surprisingly, the defects are largest in magnitude for the extremely long-lived states $u = (6, 24), (6, 29)$, and $(3, 32)$ where the critical density is effectively zero. However, even in these cases, the cancellation in equation (19) is not complete, and the QB state contributes to the effective TBR rate constant. For the other QB states, the typical value $\delta_u^{max} = -0.5$ shows that the QB contribution would be at most reduced in half at high densities. It is also noteworthy that the high density limit tends to move the system toward the LTE limit, so the $\delta_b = -1$ assumption is really too severe. The IOS approximation is not appropriate for computing the bound-bound transitions needed to determine accurate values of the δ_b due to the large internal energy spacing [22]. However, several master equation studies of CID for $\text{H} + \text{H}_2$ in astrophysical environments [33–35] have shown that it is only at very low densities that non-LTE behavior would be important and the $\delta_b = -1$ assumption would be valid, and in this case only for the highly excited states. The bound levels thermalize progressively with increasing gas density with the higher excited states thermalizing later due to the larger

radiative transition probabilities. Models of primordial star formation [36] have shown that all bound and continuum states are thermalized at densities around 10^{13} cm^{-3} . This density is less than many of the critical densities given in Tables I and II. Therefore, the falloff due to the removal of QB state contributions from the pathway-independent part of the rate constant (19) is likely to be very small for these resonances.

The results of the IOS approximation were benchmarked against the more accurate CS approximation to determine the temperature regime where they may be considered to be reliable. In both cases, the renormalized Numerov method [37] was used for propagation over R with a step size of 0.01 a.u. and a matching radius of 50 a.u. In the CS calculations, the PES was expanded in Legendre polynomials with truncation limit $\lambda_{max} = 10$. Likewise, in the IOS calculations, a Legendre expansion was used for the T-matrix with the same value of λ_{max} . A 40-point Gaussian quadrature was used to integrate over θ with only 20 angles needed in the computations due to homonuclear symmetry. We used $l_{max} = 10$ for collision energies between 1 and 10 cm^{-1} , $l_{max} = 30$ for energies between 10 and 100 cm^{-1} , $l_{max} = 60$ for energies between 100 and 1,000 cm^{-1} , $l_{max} = 120$ for energies between 1,000 and 10,000 cm^{-1} , and $l_{max} = 200$ for energies between 10,000 and 100,000 cm^{-1} . This wide energy grid and a small energy step-size ensured that the Boltzman average in equation (13) contained negligible interpolation and truncation error.

For the CS calculations performed in the present work, we extended the temperature range of previous calculations [5] using the scale parameters given by Ohlinger et al. [38]. These scale factors increase with j in order to get a good representation of the QB states and to increase the spacing between the positive energies. This reduces the amount of vibrational coupling and allows the calculations to be more tractable, however, it introduces some numerical error in the Sturmian evaluation of Q_T (see Figure 1a) which limits the reliability of the results, particularly at low temperatures. In the IOS calculations, the vibrational motion was decoupled from the dynamics, so the efficiency of the computations did not depend on the choice of scale parameter. Therefore, we were able to choose a smaller value and effectively remove this source of error from the calculations. Figure 6

shows that the CS and IOS results agree very well for temperatures greater than 600 K. In both sets of calculations, the basis sets were restricted to $j_{max} = 20$. For larger j -values, the CS calculations become too inefficient due to the increased coupling and larger number of projection quantum numbers. The IOS results for $j_{max} = 30$ illustrate the importance of the larger j -values as the temperature is increased. Although these results are very nearly converged over the entire temperature range shown, the apparent agreement with the experimental data point [10] at 300 K is not meaningful. The CS curve does appear to give a similar temperature dependence as the experimental data but with a larger magnitude. As was noted previously [5], there is significant uncertainty in the MR PES when the H-H bond is stretched which has an affect on the TBR rate constant. This is the most likely source of the discrepancy between the CS results and the experiment. In order to further explore this possibility, we tested a pairwise additive PES consisting of the He-H potential

$$v(r) = 2.2 \times 10^{-5} e^{-0.8(r-6.8)} \left[e^{-0.8(r-6.8)} - 2 \right] \quad \text{a.u.} \quad (31)$$

using the IOS approximation. For an inert collider such as He, it is expected that a pairwise additive PES would give a reasonable estimate of the TBR rate [2]. The result is shown in Figure 7 which compares the TBR rate constants computed with the two surfaces. The results do not agree particularly well at temperatures less than 10,000 K which confirms that the uncertainty in the PES is largely responsible for the discrepancy with experiment.

For H+H+H, the same basis set and numerical parameters were used as for He colliders. Therefore, the IOS approximation is estimated to be reliable above 600 K (see Figure 6). The distinguishable particle cross sections were multiplied by three in order to account for the three possible pairs of molecules that may recombine. The results are shown in Figure 8 along with the curve of Palla et al. [39] which is typically used in astrophysical models [15]. The present results are in reasonable agreement at high temperature and are within a factor of 2 of the experiment of Jacobs et al [11]. However, we find a much flatter temperature dependence with decreasing temperature than is given by the extrapolation of Palla et al. [39]. The present results are also similar to the DEB quasiclassical calculations of Esposito and Capitelli [14]. Their DEB label refers to detailed balance applied to direct

CID from bound states. Classical calculations do not distinguish between the free and interacting continuum, and it was assumed that direct dissociation involves exclusively the free continuum [14]. If this interpretation is correct, then upon application of detailed balance, the DEB curve would correspond most closely to the k_r^0 rate, which as we have argued is the same as the pathway-independent rate. In separate calculations, Esposito and Capitelli performed classical dynamics calculations of the ORT contributions for both the ET and Ex mechanisms. The results of these calculations were then added to the DEB results assuming a temperature over pressure ratio of 3000 (which corresponds to $[H]=2.4 \times 10^{18} \text{ cm}^{-3}$) and improved agreement with the experiment of Jacobs et al [11] was found. Because no master equation analysis was performed to justify this addition (and based on our analysis, it is expected to give a negative rather than positive contribution) we believe it is better to compare only against their DEB result. The similarity between the classical DEB result and the quantum mechanical IOS result is very encouraging and shows that the temperature dependent fit [39] does not reliably extrapolate to lower temperatures. This conclusion is further strengthened by the insensitivity of the classical calculations [14] to the BKMP2 versus LSTH surfaces. It is also noteworthy that the experimental data of Jacobs et al. [11] were based on shock tube measurements of CID which produced results that were not claimed to be of high accuracy. In fact, the results were in the middle of a range of reported values that scattered over an order of magnitude. Considering this uncertainty and the approximate treatment of the dynamics in the theoretical calculations, it is difficult to say which result is the most reliable. Nevertheless, it appears that some of the uncertainty in the TBR rate constant used in astrophysical models may be removed [40]. The present results, the experimental data [11], and the classical DEB results [14], are all within a factor of 2 for temperatures in the experimental range 2900-4700 K, and the two theoretical calculations are within a factor of 2 for all temperatures above 300 K. Therefore, the factor of ~ 100 uncertainty which was introduced by various extrapolation methods [15] would be reduced to a factor of ~ 2 when either the present or DEB results are used to estimate the TBR rate at the temperatures required by the astrophysical simulations [40].

IV. CONCLUSIONS

In the well-known resonance theory of molecule formation, the main quantum feature is the identification of the appropriate collision complex [2]. The QB orbiting resonances are generally used to identify two-step mechanisms for recombination, and classical or quantum mechanical calculations are then used to describe the dynamics. Results from the different two-step mechanisms are then typically [9,13] added together to obtain the total TBR rate.

Although the ORT is still in wide use, it has been shown that non-resonant processes are generally not negligible, and in many instances provide the dominant contribution to the TBR rate [6,7]. Adding the various contributions together may lead to double counting of the kind pointed out by Wei, Alavi, and Snider [4] who showed that each mechanism must give the same result when the calculations are carried out exactly. The quantum calculations of Pack, Walker, and Kendrick [1] do not suffer the double counting problem, however, their interpretation of the various mechanisms differs from [4] in that it does not distinguish between the free continuum and the BAB resonant and non-resonant part of the interacting continuum. This leads to a definition of the recombination rate k_r which is slightly different from the pathway invariant definition given in [3,4]. Nevertheless, the results of their master equation analysis show very similar behavior to the steady-state solution of the Sturmian theory given here. The classical calculations of Esposito and Capitelli [14] also do not distinguish between the free continuum and the BAB resonant and non-resonant part of the interacting continuum. These calculations carefully added together the ORT contributions with a direct recombination piece, but it is difficult to know for certain whether any double counting has occurred. The present calculations show better agreement with their DEB result, which we interpret as a classical calculation (computed using the direct mechanism) of the pathway-independent part of the phenomenological rate constant.

The Sturmian theory provides a practical implementation of the quantum kinetic theory of Snider and Lowry [3]. Unlike ORT which uses energy and lifetime and considerations to select the most important QB states (sometimes called RBC states) for recombination, the Sturmian theory retains all unbound states for a given mechanism. Calculations are

performed for a single mechanism only, and the result is considered to be the complete TBR rate in the LTE limit. For non-LTE systems, the QB states may be treated as distinct species and the pathway dependence of their formation may be incorporated via solution of a set of master equations. We have estimated that non-LTE corrections are typically small compared to the pathway-independent contribution. In the absence of a full master equation analysis, it is recommended that only the pathway-independent rate coefficients be used to estimate the effective rates.

The ET mechanism was used in the present work, however, alternate implementations are certainly possible. For example, if one wished to formulate the theory in terms of the direct process (2), then the Sturmian representation used in the dynamics would need to be for the free AB continuum rather than the interacting $A \cdots B$ subsystem used here. The dynamical calculations would perhaps be more difficult to solve since the transition operator T_0 acting on the free Sturmian basis set would not be of the usual $V + VGV$ form. Likewise, the exchange process (4) would require a Sturmian representation of the $A \cdots C$ subsystem followed by a dynamical calculation of the rearrangement, presumably a calculation of greater difficulty than the single arrangement dynamics considered here.

The present numerical study has shown how to apply the Sturmian theory at relatively high temperatures where multiple scattering and interference effects are largely negligible. These calculations are sufficient to address the uncertainties that are currently limiting astrophysical simulations of primordial star formation [15]. The same framework, however, should be applicable at intermediate temperatures with an improved quantum mechanical description of the dynamics. The simplified IOS approximation [21] may be extended to include vibrational coupling in the usual way [20]. This would increase the computational effort by requiring a large number of vibrational basis functions to be coupled together in the dynamical calculation. For the H+H+H system, it is likely that all of the 101 vibrational functions used in the Sturmian representation would need to be coupled together for each orientation angle. This would still be a manageable calculation using modern computers.

At low temperatures, the methods described here would need to be further developed.

The IOS approximation breaks down and should be replaced by the CS approximation or even the full CC formulation. For systems which contain an inert gas, such as He+H+H and Ar+H+H, the CS approximation has been used with a Sturmian representation of the ET mechanism to describe the TBR [5]. The results appear to give the correct temperature dependence but are inconclusive due to uncertainties in the potential energy surfaces. For systems which support bound states in more than one arrangement, there would likely be interference between the different mechanisms at low temperatures, and a more sophisticated quantum dynamical calculation [41–45] would be required.

Acknowledgments

This work was supported by the NSF grant No. PHY-1203228. The author would like to thank Dr. Brian Kendrick for a careful reading of the manuscript and Dr. Nicolais Guevara for providing the He-H potential used in this work.

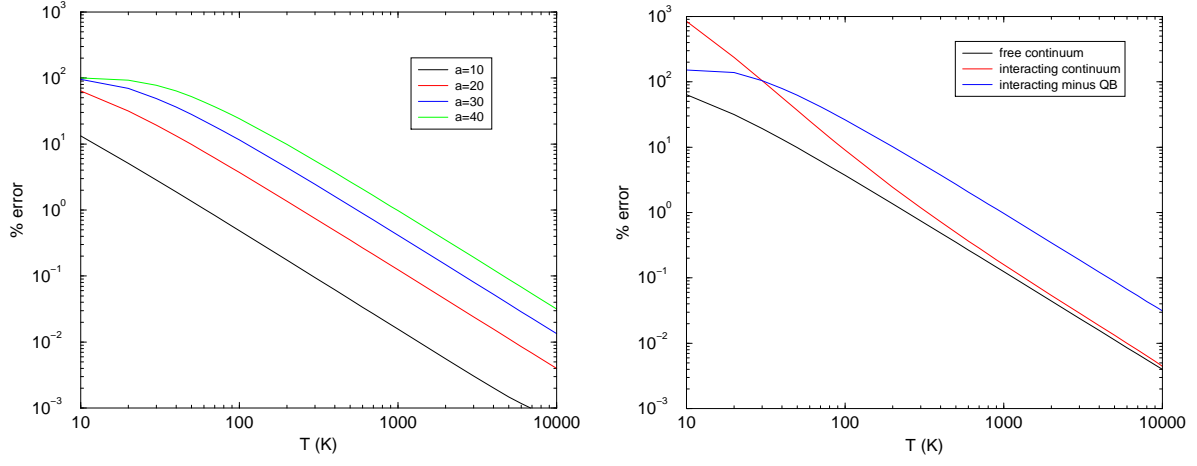


Figure 1: Percent error in the translational partition function Q_T computed using the Sturmian eigenvalues for $j = 4$. (a) Free particle interaction with different values of scale parameter; (b) Interacting continuum with and without the long-lived QB state included in the representation. These calculations used $a = 20$.

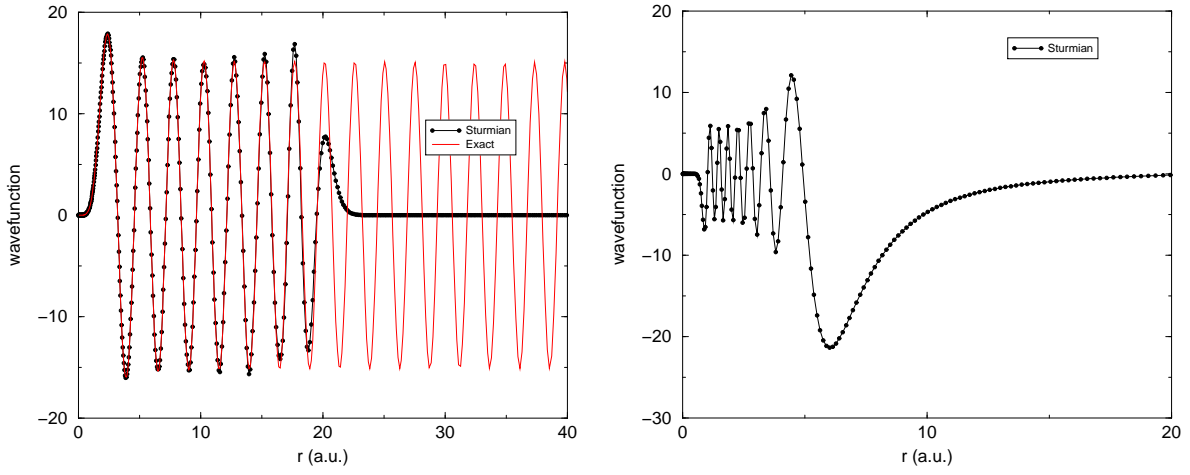


Figure 2: Sturmian representation of $j = 4$ eigenstates for (a) free continuum and (b) interacting continuum. In both cases, the 14th vibrational eigenstate is plotted for $a = 20$. This choice of scale factor causes all of the continuum eigenstates to go to zero for interatomic distances greater than 25 a.u. The interacting eigenstate corresponds to a QB resonance with an energy of 0.9 cm^{-1} and a width of $8.4 \times 10^{-6} \text{ cm}^{-1}$.

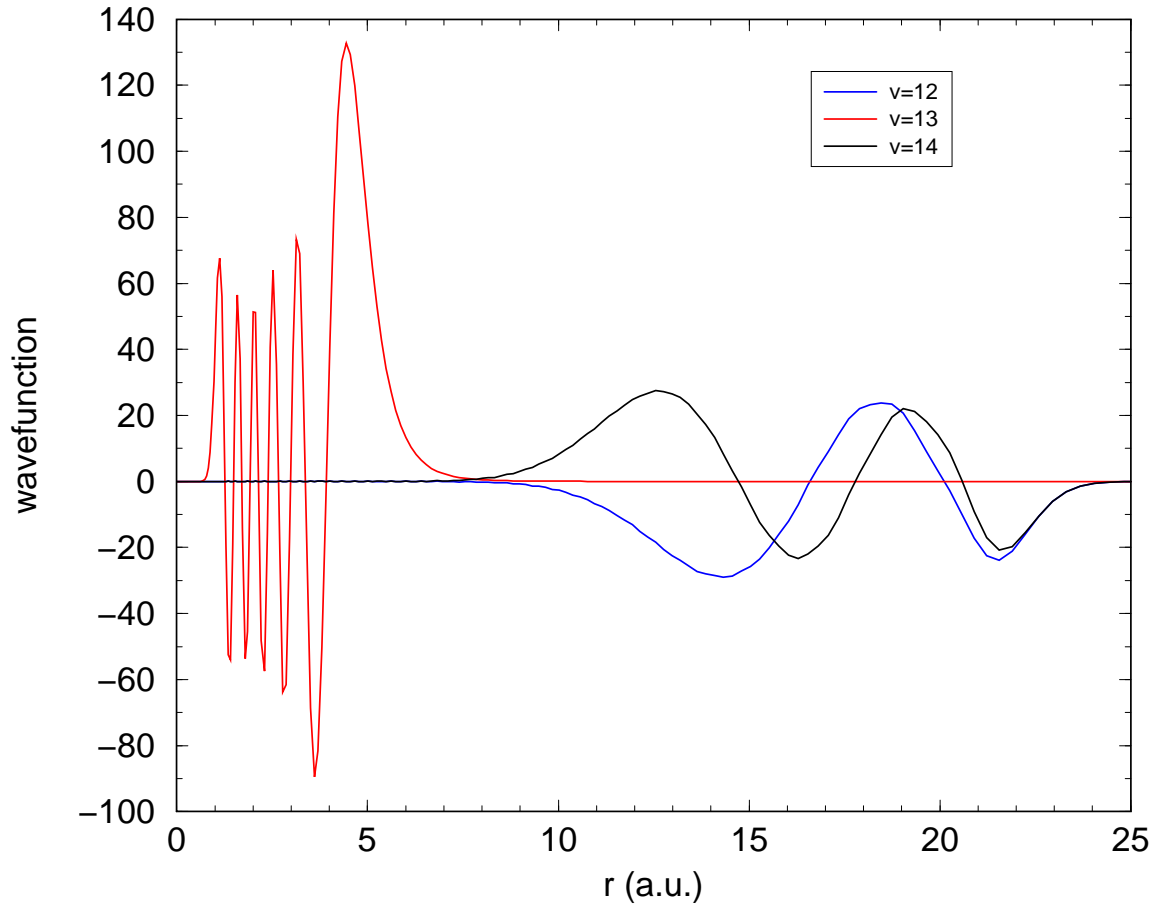


Figure 3: Sturmian representation of the $j = 15$ interacting continuum eigenstates for $v = 12 - 14$ using a scale factor $a = 20$. The $v = 13$ eigenstate corresponds to a QB resonance with a width of $3.2 \times 10^{-6} \text{ cm}^{-1}$. The figure shows there is negligible coupling between the resonance and the neighboring continuum states. Higher vibrational levels do show overlap and can help keep the QB concentration from being depleted.

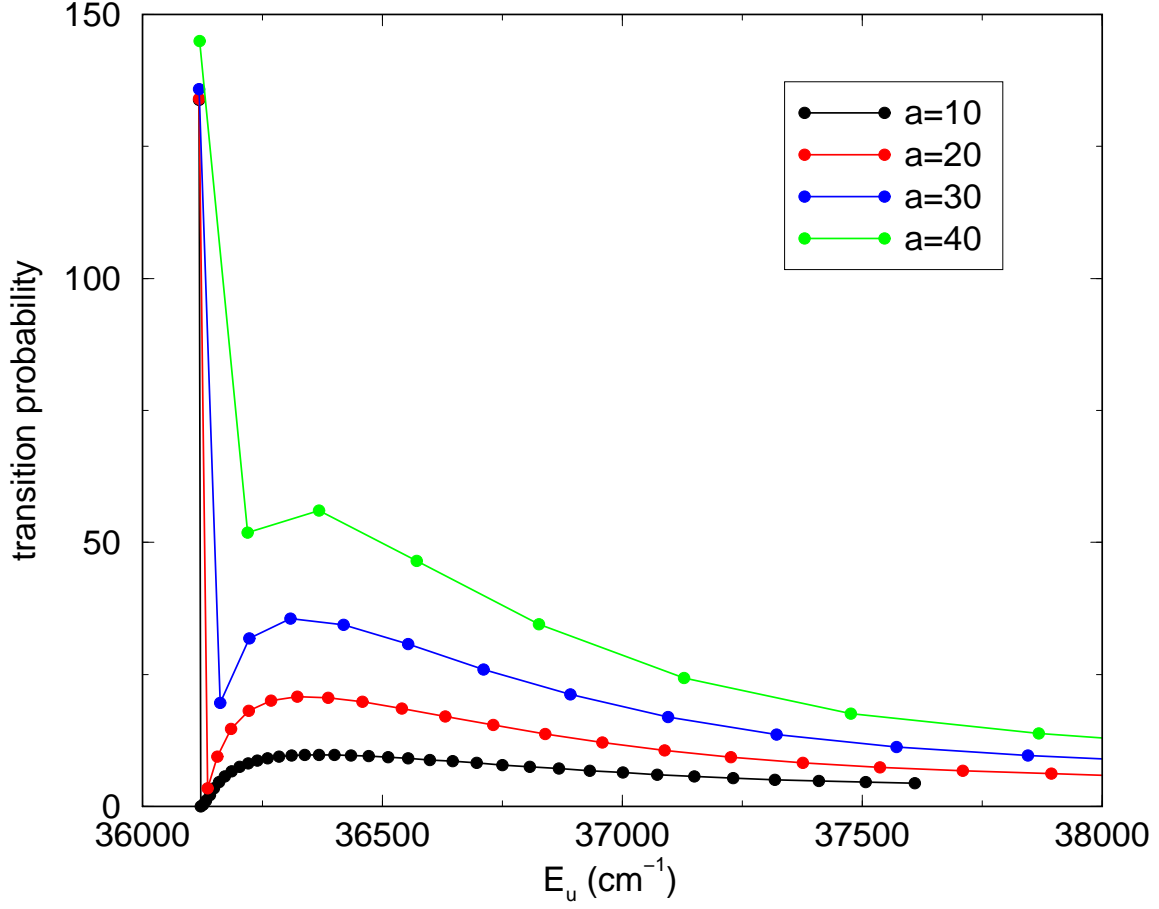


Figure 4: Cumulative bound-free transition probability as a function of Sturmiian energy and scale parameter. The calculations are for $\text{He}+\text{H} \cdot \cdot \text{H}(j=4)$ computed with the MR PES. The scale dependence is due to the unit normalization of the Sturmiian basis set. The energy normalization cancels with the equivalent quadrature weights for the sum over f and allows the sum over u to be obtained by simply adding the values at the points shown in the figure. For example, the sum over u for $E_u < 37,500 \text{ cm}^{-1}$ yields 366.49, 366.43, 365.93, and 375.72 for the respective curves $a=10, 20, 30$, and 40 . The IOS approximations was used for these calculations with $E_T = 100 \text{ cm}^{-1}$ and $J_{max} = 30$.

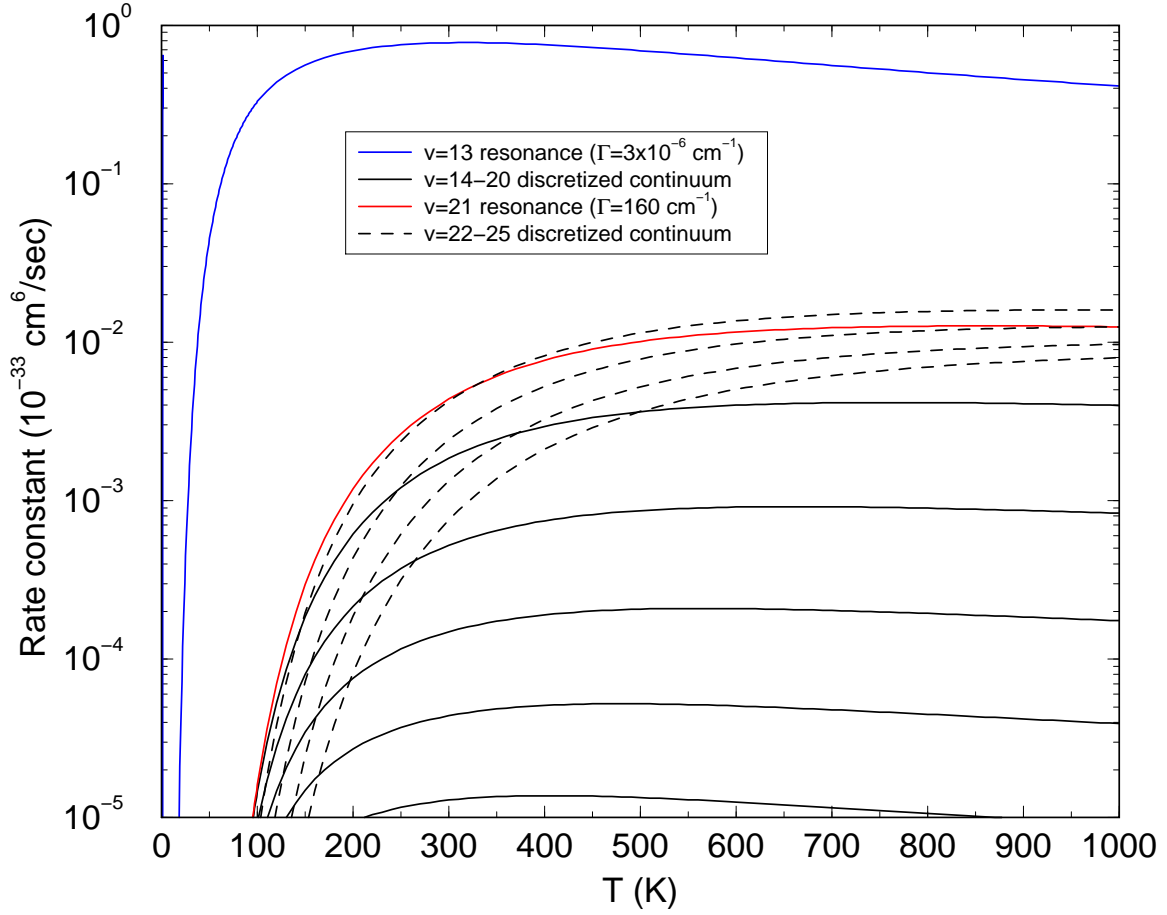


Figure 5: TBR partial rate constants for $\text{He}+\text{H} \cdot \cdot \text{H}(j = 15)$ computed with the MR PES. Each curve includes a sum over all bound levels. The resonant contributions are shown in blue (QB) and red (BAB), and the non-resonant contributions are shown as solid lines (low energies) and dashed lines (high energies).

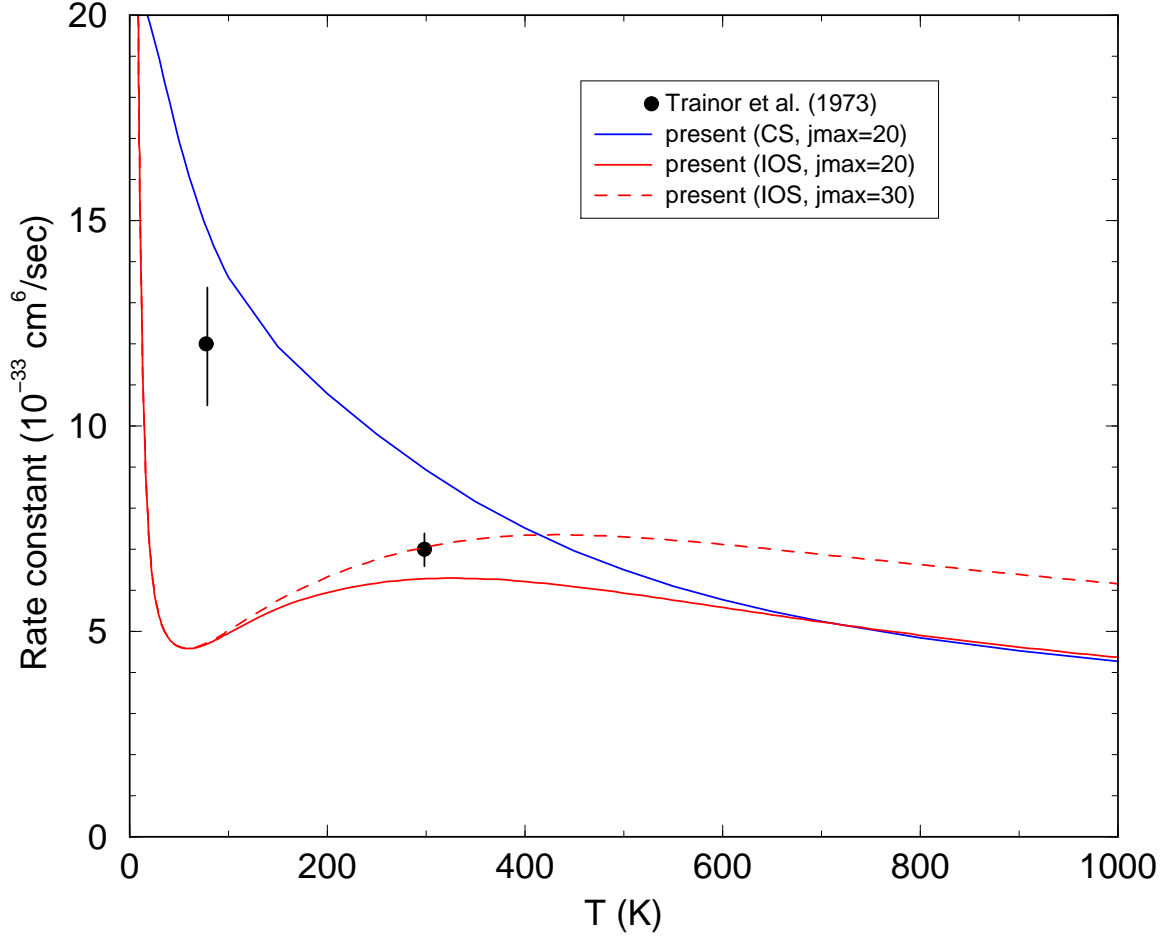


Figure 6: TBR rate constant for $\text{He}+\text{H}+\text{H}$ computed with the MR PES. The CS result (blue curve) appears to give a similar temperature dependence as the experimental data points but with a larger magnitude. When the same $j_{\text{max}} = 20$ condition is used, the IOS result (solid red curve) and the CS result show good agreement for temperatures above 600 K. The IOS result (dashed red curve) shows that $j > 20$ contribute to the TBR rate constant for $T > 100$ K.

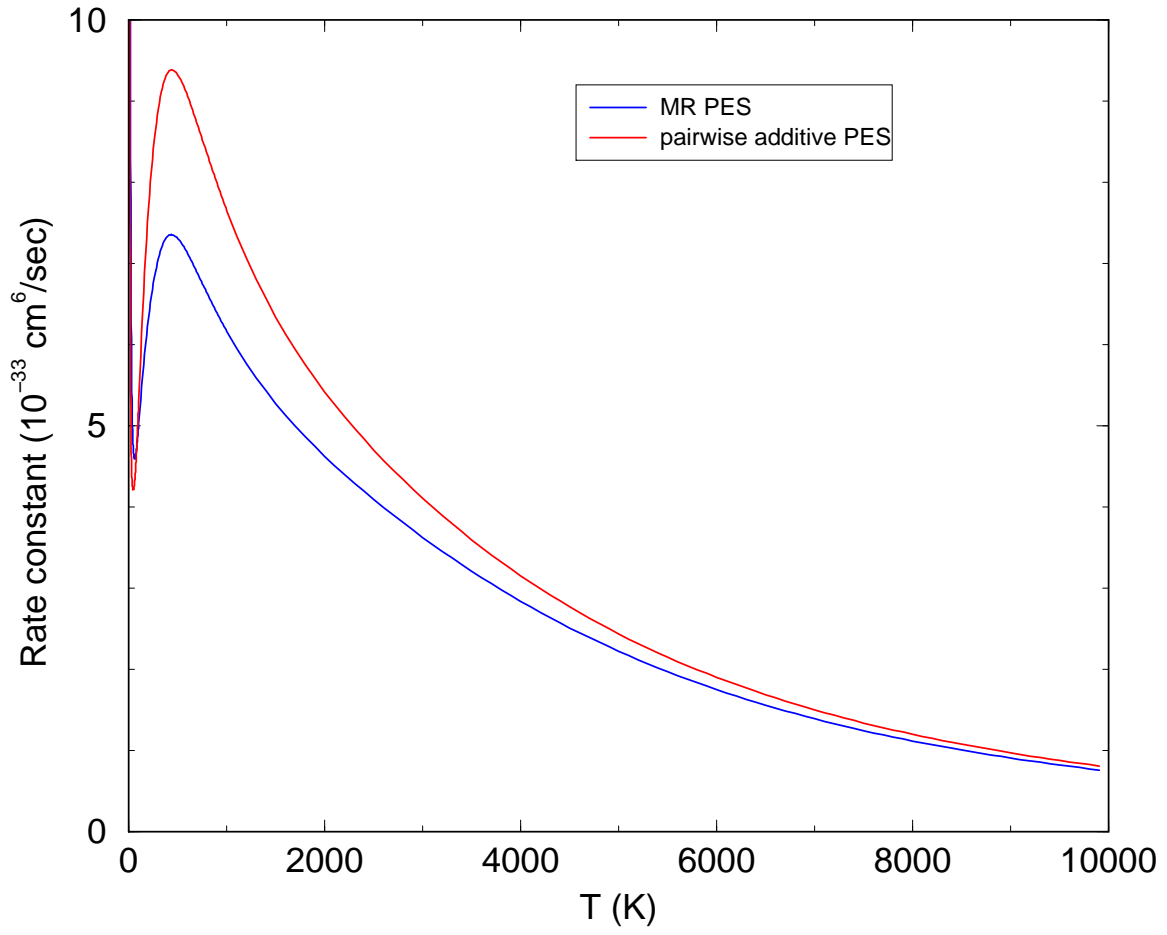


Figure 7: TBR rate constant for He+H+H computed with the MR PES [31] and a pairwise additive PES. Both calculations used the IOS approximation with $j_{max} = 30$. The three-body terms in the MR PES and the associated uncertainty at large- r produce a significant difference in the TBR rate for $T < 10,000$ K.

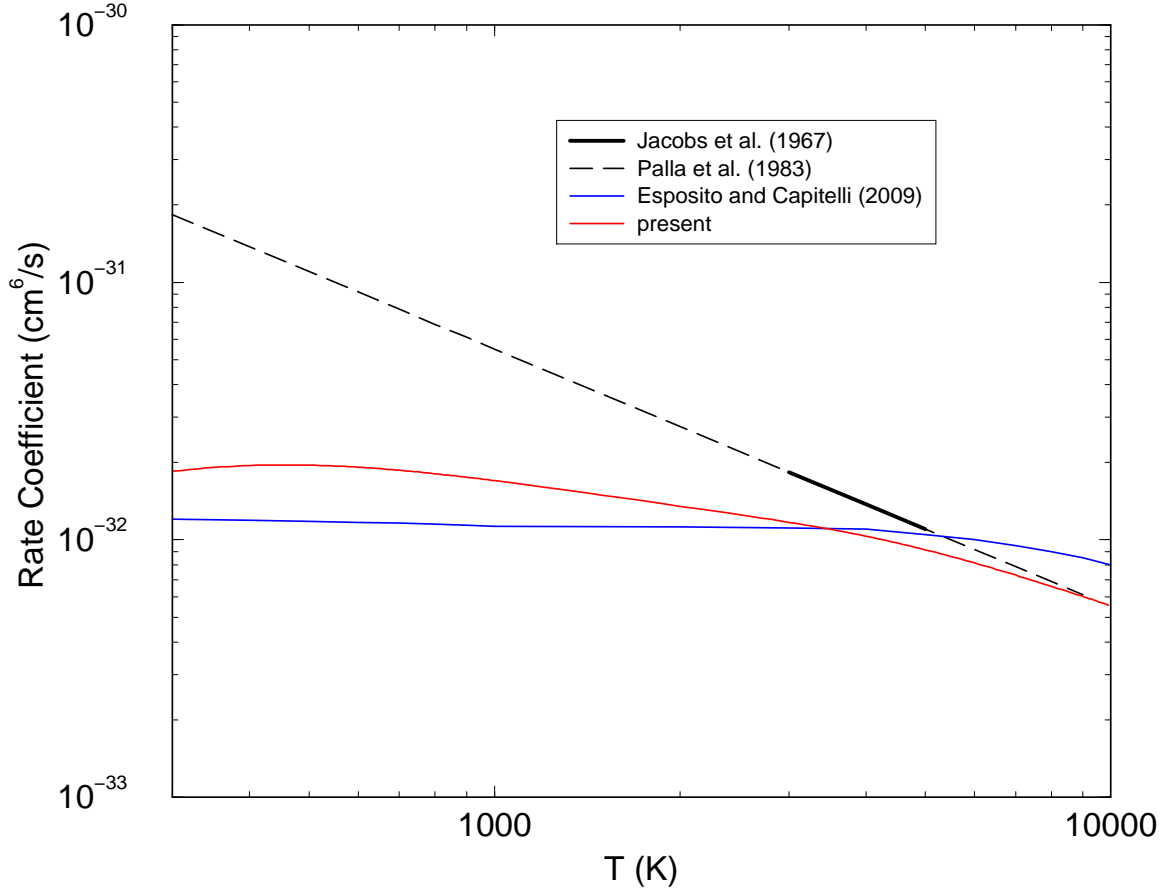


Figure 8: TBR rate constant for $\text{H}+\text{H}+\text{H}$ computed with the BKMP2 PES using the IOS approximation with $j_{max} = 35$. The present results and the quasiclassical DEB results of Esposito and Capitelli [14] show a much flatter temperature dependence than the extrapolated curve of Palla et al [39] which is based on the experimental data of Jacobs et al [11].

TABLES

TABLE I. Resonance parameters for para-H₂($X^1\Sigma_g^+$) at $T = 1000$ K

$u = (v, j)$	τ_u (s)	$\sum_b k_{u \rightarrow b}$ (cm ³ s ⁻¹)	$\sum_{u'} k_{u \rightarrow u'}$ (cm ³ s ⁻¹)	[He] _{cr} (cm ⁻³)	δ_u^{max}
(14,4)	6.3×10^{-7}	1.3×10^{-9}	4.0×10^{-9}	3.0×10^{14}	-0.25
(6,24)	4.8×10^9	1.0×10^{-8}	4.7×10^{-9}	0	-0.69
(10,26)	2.8×10^3	8.2×10^{-9}	7.0×10^{-9}	2.4×10^4	-0.54
(14,28)	2.5×10^0	8.0×10^{-9}	7.3×10^{-9}	2.6×10^7	-0.52
(17,30)	3.8×10^{-2}	8.0×10^{-9}	6.1×10^{-9}	1.9×10^9	-0.57
(3,32)	8.8×10^{21}	8.7×10^{-9}	1.2×10^{-9}	0	-0.88
(21,32)	3.0×10^{-3}	7.7×10^{-9}	5.5×10^{-9}	2.6×10^{10}	-0.58
(24,34)	9.7×10^{-4}	2.5×10^{-9}	9.3×10^{-9}	8.8×10^{10}	-0.21

TABLE II. Resonance parameters for ortho- $\text{H}_2(X^1\Sigma_g^+)$ at $T = 1000$ K

$u = (v, j)$	τ_u (s)	$\sum_b k_{u \rightarrow b}$ (cm^3s^{-1})	$\sum_{u'} k_{u \rightarrow u'}$ (cm^3s^{-1})	$[\text{He}]_{cr}$ (cm^{-3})	δ_u^{max}
(14,13)	1.3×10^{-9}	5.2×10^{-9}	7.8×10^{-9}	5.9×10^{16}	-0.40
(13,15)	1.7×10^{-6}	6.1×10^{-9}	7.7×10^{-9}	4.3×10^{13}	-0.44
(12,17)	1.5×10^{-4}	6.6×10^{-9}	7.9×10^{-9}	4.6×10^{11}	-0.46
(12,19)	4.1×10^{-4}	7.0×10^{-9}	8.3×10^{-9}	1.6×10^{11}	-0.46
(13,21)	1.4×10^{-4}	7.3×10^{-9}	8.6×10^{-9}	4.5×10^{11}	-0.46
(15,23)	2.4×10^{-5}	7.6×10^{-9}	8.9×10^{-9}	2.5×10^{12}	-0.46
(17,25)	4.1×10^{-6}	7.8×10^{-9}	8.6×10^{-9}	1.5×10^{13}	-0.47
(20,27)	7.7×10^{-7}	7.8×10^{-9}	8.6×10^{-9}	7.9×10^{13}	-0.47
(6,29)	6.5×10^{12}	1.0×10^{-8}	3.0×10^{-9}	0	-0.78
(22,29)	2.0×10^{-7}	6.9×10^{-9}	9.5×10^{-9}	3.0×10^{14}	-0.42
(11,31)	3.5×10^6	8.2×10^{-9}	4.1×10^{-9}	2.3×10^1	-0.67
(25,31)	8.0×10^{-8}	3.7×10^{-9}	1.2×10^{-8}	7.8×10^{14}	-0.23
(16,33)	6.0×10^3	8.2×10^{-9}	2.6×10^{-9}	1.6×10^4	-0.76
(27,33)	5.3×10^{-8}	2.1×10^{-9}	1.2×10^{-8}	1.3×10^{15}	-0.15
(30,35)	6.4×10^{-8}	1.8×10^{-9}	1.1×10^{-8}	1.2×10^{15}	-0.14

REFERENCES

- [1] R. T. Pack, R. B. Walker, and B. K. Kendrick, J. Chem. Phys. **109**, 6701 (1998).
- [2] R. E. Roberts, R. B. Bernstein, and C. F. Curtiss, J. Chem. Phys. **50**, 5163 (1969).
- [3] R. F. Snider and J. T. Lowry, J. Chem. Phys. **61**, 2330 (1974).
- [4] G. W. Wei, S. Alavi, and R. F. Snider, J. Chem. Phys. **106**, 1463 (1997).
- [5] S. Paolini, L. Ohlinger, and R. C. Forrey, Physical Review A **83**, 042713 (2011).
- [6] R. T. Pack, R. B. Walker, and B. K. Kendrick, J. Chem. Phys. **109**, 6714 (1998).
- [7] D. W. Schwenke, J. Chem. Phys. **92**, 7267 (1990).
- [8] J. Troe, Phys. Chem. **6B**, 835 (1975).
- [9] P. A. Whitlock, J. T. Muckerman, and R. E. Roberts, J. Chem. Phys. **60**, 3658 (1974).
- [10] D. W. Trainor, D. O. Ham, and F. Kauffman, J. Chem. Phys. **58**, 4599 (1973).
- [11] T. A. Jacobs, R. R. Giedt, and N. Cohen, J. Chem. Phys. **47**, 54 (1967).
- [12] D. G. Truhlar, Ann. Rev. Phys. Chem. **27**, 1 (1976).
- [13] A. E. Orel, Journal of Chemical Physics **87**, 314 (1987).
- [14] F. Esposito and M. Capitelli, J. Phys. Chem. A **113**, 15307 (2009).
- [15] M. J. Turk, P. Clark, S. C. O. Glover, T. H. Greif, T. Abel, R. Klessen, and V. Bromm, Astrophysical Journal **726**, 55 (2011).
- [16] E. J. Heller, W. P. Reinhardt, and H. A. Yamani, J. Comp. Phys. **13**, 536 (1973).
- [17] R. T. Pack, J. Chem. Phys. **60**, 633 (1974).
- [18] P. McGuire and D. J. Kouri, J. Chem. Phys. **60**, 2488 (1974).
- [19] P. McGuire, J. Chem. Phys. **62**, 525 (1975).
- [20] G. A. Parker and R. T. Pack, J. Chem. Phys. **68**, 1585 (1978).

- [21] G. A. Pfeffer, J. Phys. Chem. **89**, 1131 (1985).
- [22] K. Sakimoto, J. Phys. B **30**, 3881 (1997).
- [23] V. Khare, D. J. Kouri, and M. Baer, J. Chem. Phys. **71**, 1188 (1979).
- [24] D. J. Kouri, V. Khare, and M. Baer, J. Chem. Phys. **75**, 1179 (1981).
- [25] J. M. Bowman and K. T. Lee, J. Chem. Phys. **72**, 5071 (1980).
- [26] B. M. D. D. Jansen op de Haar and G. Balint-Kurti, J. Chem. Phys. **85**, 2614 (1986).
- [27] R. M. Whitnell and J. C. Light, J. Chem. Phys. **86**, 2007 (1987).
- [28] M. Baer, C. Y. Ng, and D. Neuhauser, Chem. Phys. Lett. **169**, 534 (1990).
- [29] D. W. Schwenke, J. Chem. Phys. **89**, 2076 (1988).
- [30] D. W. Schwenke, Theor. Chim. Acta **74**, 381 (1988).
- [31] P. Muchnick and A. Russek, J. Chem. Phys. **100**, 4336 (1994).
- [32] A. I. Boothroyd, P. G. Martin, W. J. Keogh, and M. J. Peterson, J. Chem. Phys. **116**, 666 (2002).
- [33] W. Roberge and A. Dalgarno, Astrophysical Journal **255**, 176 (1982).
- [34] S. Lepp and J. M. Shull, Astrophysical Journal **270**, 578 (1983).
- [35] P. G. Martin, D. H. Schwarz, and M. E. Mandy, Astrophysical Journal **461**, 265 (1996).
- [36] D. R. Flower and G. J. Harris, Mon. Not. R. Astron. Soc. **377**, 705 (2007).
- [37] J. P. Leroy and R. Wallace, J. Phys. Chem. **89**, 1928 (1985).
- [38] L. Ohlinger, R. C. Forrey, T.-G. Lee, and P. C. Stancil, Phys. Rev. A **76**, 042712 (2007).
- [39] F. Palla, E. E. Salpeter, and S. W. Stahler, Astrophysical Journal **271**, 632 (1983).
- [40] R. C. Forrey, *Rate of three-body recombination of hydrogen molecules during primordial star formation*, arXiv: 1306.5163 (2013).
- [41] G. A. Parker, R. B. Walker, B. K. Kendrick, and R. T. Pack, J. Chem. Phys. **117**, 6083 (2002).

- [42] F. D. Colavecchia¹, F. Mrugala, G. A. Parker, and R. T Pack, J. Chem. Phys. **118**, 10387 (2003).
- [43] B. D. Esry, C. H. Greene, and J. P. Burke, Jr., Phys. Rev. Lett. 83, 1751 (1999).
- [44] H. Suno, B. D. Esry, C. H. Greene, and J. P. Burke, Jr., Phys. Rev. A 65, 042725 (2002).
- [45] H. Suno and B. D. Esry, Phys. Rev. A 80, 062702 (2009).